Evolutionary Ecology Research, 2006, **8**: 1333–1347

The evolution of parasite dispersal, transmission, and virulence in spatial host populations

Masashi Kamo[1]* and Mike Boots[2]

[1]*Advanced Industrial Science and Technology, Research Centre for Chemical Risk Management, Onogawa 16-1, Tsukuba, Ibaraki 305-8569, Japan and* [2]*Department of Animal and Plant Sciences, University of Sheffield, Sheffield, UK*

ABSTRACT

Questions: How does parasite dispersal evolve? What is the impact of the evolution of parasite dispersal on the evolution of transmission and virulence?

Mathematical methods: Spatially explicit host parasite models with local and global interactions, analysed by pair approximation and simulation. Pairwise invasibility plots.

Key assumptions: Infected and susceptible hosts are arranged on a regular lattice. Infection can occur locally or globally with some probability. The proportion of long-distance infection and parasite life-history traits evolve by small mutations between haploid strains. There is no explicit cost to long-distance dispersal.

Conclusions: An intermediate degree of long-distance infection always evolves. This is due to a balance between the advantages from long-distance dispersal (avoiding local competition for susceptible hosts) and costs to dispersal (that emerge from the spatial heterogeneity of the hosts). Evolution maximizes parasite transmission rate in a spatially structured host population when parasite dispersal can also evolve. The evolution of parasite dispersal may lead to the concurrent evolution of higher parasite transmission and virulence than found in completely mixed populations. Interactions between the completely local and global are therefore important.

Keywords: disease, dispersal, evolution, evolutionarily stable strategy, models, parasites, spatial.

INTRODUCTION

In natural host–parasite interactions, very little is known about the potential of parasites to evolve different dispersal rates (Perez-Tris and Bensch, 2005). There is, however, considerable evidence that parasites may manipulate their hosts (see Poulin, 1994, 1995) and they therefore have the potential to alter their dispersal since they often disperse with their infected hosts. Different parasite transmission strategies will often alter parasite dispersal distance, with extreme examples being the evolution of a water-borne or indeed vector-borne infection (Ewald, 1994). In addition, key parasite life-history traits such as transmission and virulence

* Author to whom all correspondence should be addressed. e-mail: masashi-kamo@aist.go.jp

may evolve in a context where the proportion of local and global infection that occurs also varies due to evolution. In this paper, we examine the evolution of parasite dispersal and life history taking into account these feedbacks by using a spatially explicit modelling approach.

Classical host–parasite evolutionary theory assumes that the host population is completely mixed and therefore any individual is as likely to infect any one individual as any other. Within this framework, models of the evolution of parasites with baseline assumptions, which exclude factors such as multiple infections, predict that selection will tend to maximize the parasite's epidemiological R_0 (May and Anderson, 1983; Bremermann and Thieme, 1989). Evolution should therefore maximize the transmission rate and minimize virulence and recovery. However, a trade-off from the point of view of the parasite between transmission and virulence is generally assumed, where higher transmission can only be 'bought' at the expense of higher virulence. This trade-off results from the idea that increased growth rates of the parasite will cause more damage to the host, but also lead to the production of more infective particles and therefore higher transmission (Mackinnon and Read, 1999). If transmission is increasingly costly in terms of virulence, models predict the evolution of a finite transmission rate and virulence, otherwise evolution will maximize transmission and virulence (May and Anderson, 1983; Bremermann and Thieme, 1989).

The assumption of homogeneous mixing in host populations ignores the fact that individuals are more likely to contact and thereby infect individuals that are close to them either spatially or in social networks. One approach to examine the role of the spatial structure of individual hosts within a population is to use lattice models (also called probabilistic cellular automata, PCA) (Sato *et al.*, 1994; Rand *et al.*, 1995; Rhodes and Anderson, 1996; Boots and Sasaki, 1999; Haraguchi and Sasaki, 2000). It has been shown that the inclusion of spatial/social structure into host–parasite models may have dramatic implications for the evolution of the parasite. In particular, the transmission rate of the parasite is no longer maximized in models with local interactions (Rand *et al.*, 1995; Haraguchi and Sasaki, 2000). This is a result of 'self-shading', where parasite strains with lower transmission rates gain an advantage in terms of an increased proportion of susceptible individuals being next to infected ones and therefore available for infection.

In a broader context, the invasion fitness in spatially structured populations needs to take into account local population correlations (van Baalen and Rand 1998), since local interactions may increase competition with oneself leading to different evolutionary outcomes (Hamilton and May, 1977; Ferriere and Michod, 1995, 1996; Harada, 1999).

The assumption of complete mixing in the classical 'mean-field' models on the one hand and that only immediate neighbours interact on the other are, in fact, two ends of a continuum. In nature, most systems will have interactions that fall between these two extremes. Modelling realistic intermediate population structures, however, inevitably leads to models of higher complexity than the local or mean-field models. A tractable approach is to assume that either local or global interactions can occur. For example, Boots and Sasaki (1999) included both local and global transmission and showed that the evolutionarily stable (ES) transmission rate reduced as a higher proportion of infections were local. As such, it showed that the spatial constraint on transmission was not an artefact of the completely local interactions assumed previously (Rand *et al.*, 1995). The characterization of interactions as either completely local or random can also be argued to be a reasonable characterization for natural systems where most individuals tend either to remain locally or disperse.

In contrast, some systems may vary in the distance that they disperse, which is perhaps most realistically modelled in continuous space (Bolker and Pacala, 1997, 1999; Bolker, 1999, 2003; Murrell *et al.*, 2001, 2002, 2004), where the location of each individual is tracked. However, the resulting moment equations of these models are partial or integro differential equations, and are therefore much less amenable to analysis. In addition, Ellner (2001) has developed a multi-scale pair approximation which suggests that it is usually sufficient to approximate all but the shortest-range interactions by a global interaction. Varying the proportion of local and global interactions is therefore likely to be a useful method of modelling population structure in a range of circumstances.

Here we model spatial host dynamics where infection occurs at some proportion of local and global and this proportion is allowed to evolve. Our approach is a combination of Monte-Carlo simulation and the analysis of pair approximations in an adaptive dynamics framework. We assume that reproduction is always local and, as a consequence, the host population is spatially structured. Optimal dispersal is clearly a balance between its costs and benefits. However, we do not assume any costs or benefits of dispersal explicitly. The spatial epidemiological dynamics themselves lead to benefits from the avoidance of 'self-shading', but also lead to costs due to the heterogeneity of the susceptible hosts. We show that there is an optimal propensity to disperse even though no costs to global dispersal are assumed. In addition, we examine the evolution of parasite transmission and virulence when dispersal is also evolving and show that they are both maximized at the optimal dispersal.

MATERIALS AND METHODS

We consider a regular network of sites, each of which corresponds to either an individual host or an empty site. There are three possible states to each site: empty (O), occupied by a susceptible (S), or occupied by an infected (I). We assume that reproduction is always local, but that transmission occurs both locally and globally by the proportion $(1-L)$ and $L\,(0 \leq L \leq 1)$, respectively. The analysis is based on ordinary pair approximation (Matsuda *et al.*, 1992; Sato *et al.*, 1994) and Monte Carlo simulation. In the simulation, a 100×100 regular square lattice with a periodic boundary is assumed. We assume a von Neumann neighbourhood, with each site having 4 neighbours. A site occupied by a susceptible individual becomes empty due to natural death at rate d and the susceptible individual becomes infected through local transmission at a rate $k\beta/4$, where β is a transmission rate and k is the number of neighbouring sites occupied by an infected individual. Global transmission occurs at a rate $\beta\rho_I$, where ρ_I is the global density of infected individuals [total transmission occurs at a rate $\beta\{L\rho_I + (1-L)k/4\}$]. Sites occupied by an infected individual (I) become empty due to death at rate $\alpha + d$, where α is an enhanced death rate due to infection (virulence). An empty site may be occupied by a susceptible individual by reproduction at a rate $kr/4$, where r is the reproduction rate and k is the number of susceptible neighbours.

The spatially structured host–parasite population is modelled by considering the pair densities of the host states. Our model is the same as that in Boots and Sasaki (1999) and therefore represents a simple spatially structured susceptible/infected (SI) host–parasite model with reproduction from susceptibles and infection occurring both locally and globally. We denote global densities by $\rho_\sigma(\sigma \in \{O,S,I\})$, and the probability that a randomly chosen host has state σ, and one of its randomly chosen nearest neighbours has state σ', by $P_{\sigma\sigma'}$. The conditional probability that a randomly chosen σ site has a σ' at its nearest

neighbour is denoted by $q_{\sigma'|\sigma}$, while the conditional probability that a randomly chosen nearest neighbour of a σ' σ'' pair has a σ site is given by $q_{\sigma|\sigma'\sigma''}$ (σ', $\sigma'' \in \{O,S,I\}$). Throughout this paper, we approximate the last conditional triplet density by doublet densities such that $q_{\sigma|\sigma'\sigma''} \approx q_{\sigma|\sigma'}$ for any σ, σ', and σ'' (Matsuda *et al.*, 1992; Sato *et al.*, 1994). The full system of dynamics is given in Appendix 1. By definition, the sum of the global densities is 1 ($\sum_\sigma \rho_\sigma = 1$), the sum of the doublet local densities is also 1 ($\sum_\sigma q_{\sigma|\sigma'} = 1$), and the pair densities are multiples of global and local densities such that

$$P_{\sigma\sigma'} = \rho_\sigma q_{\sigma'|\sigma} = \rho_{\sigma'} q_{\sigma|\sigma'} = P_{\sigma'\sigma} \text{ (for any } \sigma \text{ and } \sigma') \tag{1}$$

The global density of infected hosts changes in time according to

$$\dot{\rho}_I = [\beta_I \{L_I \rho_S + (1 - L_I) q_{S|I}\} - (\alpha_I + d)]\rho_I \tag{2}$$

where β_I, α_I, and L_I are the transmission rate, virulence, and proportion of global infection of the resident strain respectively. Since we will conduct an invasion analysis later, these strain-specific parameters have a subscript I for resident and J for mutant strain. We can solve the full system of the resident dynamics (equations A1) numerically.

Now we consider a mutant strain of pathogen denoted by subscript J, which invades the host–parasite population at an endemic equilibrium with the resident strain. The invasion analysis has been recently developed by Boots *et al.* (2006). The proportion of the global infection is considered to be a life-history parameter of the parasites, and therefore the mutants have a global infection proportion (L_J). The invasion analysis of the spatial model combines two processes. At the invasion phase, the density of the mutant is negligibly small and we can therefore ignore the density of mutants next to individuals infected with the resident strain, susceptibles, or empty sites (i.e. $q_{J|\sigma} \approx 0$, where $\sigma \in \{O,S,I\}$). However, the densities of each of these states next to individuals infected with the mutant strain ($q_{\sigma|J}$) is in contrast not negligible. Intuitively, this arises because with the low density of mutants at invasion, most of the susceptible individuals and those infected with the resident strain do not interact with an invading mutant. In contrast, an individual infected with the mutant strain which has just been introduced into the population often interacts with both resident infecteds and susceptibles. The colonization by the mutant starts in a locally limited area in the viscous population and therefore takes time to spread to the whole population. Before this spreading phase, the local density of the mutant reaches a 'quasi-equilibrium' within this limited area (Boots and Sasaki, 1999). For the invasion analysis, we first compute these quasi-equilibrium values by formalizing the mutant dynamics at the invasion phase. Next we consider changes in the global density of the mutant to determine the invasibility of the mutants.

It is straightforward to show that the global density of mutants follows the following equations:

$$\dot{\rho}_J = \rho_J [\beta_J \{L_J \hat{\rho}_S + (1 - L_J) \hat{q}^{\mathbf{0}}_{S|J}\} - (d + \alpha_J)] \tag{3}$$

where β_J, α_J, and L_J are the transmission rate, virulence, and the proportion of global infection of the mutants respectively. $\hat{\rho}_S$ is the equilibrium density of susceptible hosts computed by solving equations (A1) at steady state. $\hat{q}^{\mathbf{0}}_{S|J}$ is the local density of susceptible individuals in the neighbourhood of the invading mutants at a 'quasi-equilibrium' (Matsuda *et al.*, 1992; Sato *et al.*, 1994; Boots and Sasaki, 1999; Boots *et al.*, 2006). If the values inside the parentheses in equations (3) are positive, the mutants can invade, i.e. the invasion condition is

$$\lambda(J \mid I) = \beta_J \{L_J \hat{\rho}_S + (1 - L_J) \hat{q}^{\mathbf{0}}_{S|J}\} - (d + \alpha_J) \tag{4}$$

It is also straightforward to show that the pair density of mutant and empty sites, for example, changes over time as

$$\dot{P}_{OJ} = dP_{SJ} + (d+\alpha_J)P_{JJ} + (d+\alpha_I)P_{IJ} - \{(d+\alpha_J) + r(1-\theta)q_{SJOJ}\}P_{OJ} + \beta_J\{L_J\rho_J + (1-L_J)(1-\theta)q_{JJSO})\}P_{SO} \quad (5)$$

We can derive the time derivative of the conditional density from the identity relationship (equation 1). For example, if we differentiate both sides of $P_{OJ} = \rho_J q_{OJJ}$ by time, we have

$$\dot{q}_{OJJ} = \frac{1}{\rho_J}(\dot{P}_{OJ} - \dot{\rho}_J q_{OJJ}) \quad (6)$$

If we approximate the conditional triplet by the equivalent doublet (e.g. $q_{JJSO} = q_{JJS}$), and combine equations (4–6) by using equation (1), ρ_J in the denominator in equation (6) is cancelled out. Finally, we have the dynamics of q_{OJJ} as

$$\dot{q}_{OJJ} = dq_{SJJ} + (d+\alpha_I)q_{IJJ} + (d+\alpha_J)q_{JJJ} - r(1-\theta)q_{SJO}q_{OJJ} + \beta_J[L_J\rho_S + (1-L_J)(1-\theta)q_{SJJ}]q_{OJS} - \beta_J[L_J\rho_S + (1-L_J)q_{SJJ}]q_{OJJ} \quad (7)$$

Note that all the global and local densities without a subscript J are equilibrium densities computed from equations (A1) and therefore are constants. We can derive all the other time derivatives of the conditional densities of the mutants using the pair approximation and standard linearization. The full system of the mutant dynamics is given in Appendix 2. If we solve the dynamical system numerically, we obtain the quasi-equilibrium values of q_{SJJ}. Using this value and equation (4), we can determine the invasibility of the mutant.

RESULTS

We examine the evolutionary dynamics of the proportion of the global transmission rate by using pairwise invadability plots (PIPs). The PIP is a graphical representation of the evolutionary outcomes developed in the adaptive dynamical framework (Geritz *et al.*, 1997, 1998). To focus on the evolution of local to global infection, we assume that all the other parameters are shared between the strains (i.e. $\beta_I = \beta_J = \beta$, $\alpha_I = \alpha_J = \alpha$).

Evolutionarily stable proportion of global infection

Figure 1A shows four PIPs with different fixed transmission rates. In the standard way, black indicates the region where mutants can invade, while white indicates where invasion is not possible. The PIPs show that there is always a continuously stable proportion of global infection (CSS proportion). Generally, the higher the transmission rate the lower the proportion of global infection, but this effect saturates as transmission rate increases.

We confirmed these analytical results by Monte Carlo simulation. Figure 1B shows a result of the simulation with various transmission rates where each dot represents a mean of 20 replicates. In all the simulations, the mean proportion converges to a CSS proportion of global infection. As transmission rates rise, the ES global proportion converges to around $L \approx 0.5$. The ES global infection predicted by the PIPs in Fig. 1A is approximately

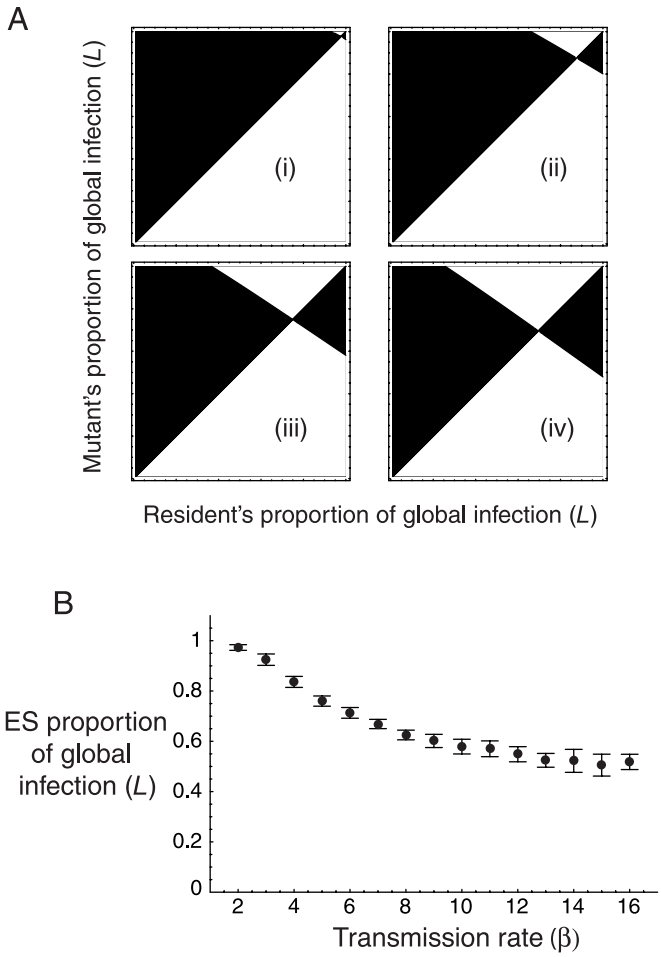

Fig. 1. (A) Pairwise invasion plots with four different transmission rates: (i) $\beta = 3$, (ii) $\beta = 5$, (iii) $\beta = 10$, and (iv) $\beta = 15$. In all panels, the vertical axes show the proportion of global infection of the mutant strain, and the horizontal axes show that of the residents, in the range $0 \leq L \leq 1$. Black indicates that the mutant strain can invade. Higher transmission rates reduce the ES global proportion, but the effect saturates as β rises. (B) Evolutionarily stable proportions computed by Monte Carlo simulation as a mean of 20 replicates at each dot. Bars indicate standard deviations. The ES proportion with high transmission is about 0.5, whereas the ES proportion predicted by PIPs with a high transmission rate is about 0.6 – indicating some inaccuracies in our approximations, possibly due to the closure of the system. However, general tendencies are well predicted by the analysis. Other parameter values are $\alpha = 1$, $d = 0.01$, $r = 3$.

0.6 with high transmission rates, and is therefore slightly different from the result of Monte Carlo simulation. This difference may be due to our assumption that environs triples approximate to their corresponding doubles in the pair approximation. The approximation does, however, capture the essential feature of the existence of a CSS global proportion of infection.

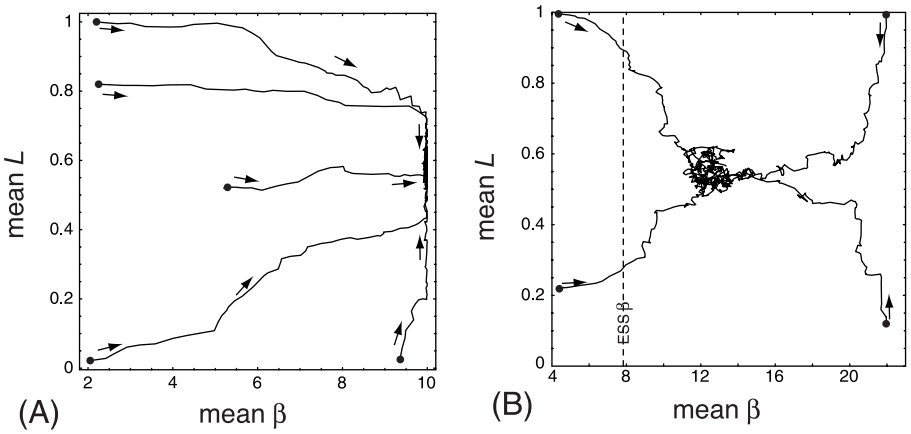

Fig. 2. Evolutionary trajectories when both transmission rate and the proportion of global transmission evolve. (A) The result when there is no trade-off between transmission rate and virulence and (B) the result when there is a trade-off. In both panels, the ES proportions of global transmission are about 0.5, and the transmission rate is maximized in (A) and about 13 in (B). A dashed line in (B) represents β, which maximizes R_0. Evolution moves away from completely mixed populations and therefore the ES transmission rate is far away from the line. Parameter values in (A) are the same as in Fig. 1 and those in (B) are C (a trade-off constant) = 20, $d = 0.1$, $r = 3$.

Evolution of both transmission rate and the proportion of global infection

Next, we allow both transmission rate and the proportion of global infection to evolve. In the well-mixed model, if the transmission rate and virulence are not linked, the highest transmission rate always evolves. Figure 2A shows the evolutionary trajectories of the transmission rate and the proportion of global transmission without any other trade-offs. In this simulation, we assumed that the maximum transmission rate is 10. In all cases, the transmission rates are maximized ($\beta = 10$) by evolution, while the proportion of global infection converges to around $L = 0.6$. This corresponds to the ES global proportion of infection when $\beta = 10$ in Fig. 1B.

Next, we examined the situation where there is a trade-off between transmission rate and virulence such that

$$\beta = C\log(1 + \alpha) \tag{8}$$

where C is a constant. This trade-off where transmission becomes acceleratingly costly in terms of virulence leads to a finite ES transmission rate in the well-mixed model. Within the spatially structured model, we find evolution to an ES proportion of global infection and an ES parasite transmission rate (Fig. 2B) that is higher than that predicted in the absence of spatial structure (indicated by a dashed line on the panel). The maximization of transmission rates and virulence at intermediate spatial structure with a saturating trade-off has been demonstrated elsewhere (Kamo *et al.*, in press). Here we have shown that the parasite will tend to evolve its dispersal such that it achieves this critical point where transmission and virulence are maximized.

Two selective processes underlie the evolution of optimal parasite dispersal. One is the role of 'self-shading' by infected individuals in their local environment. Strains with a

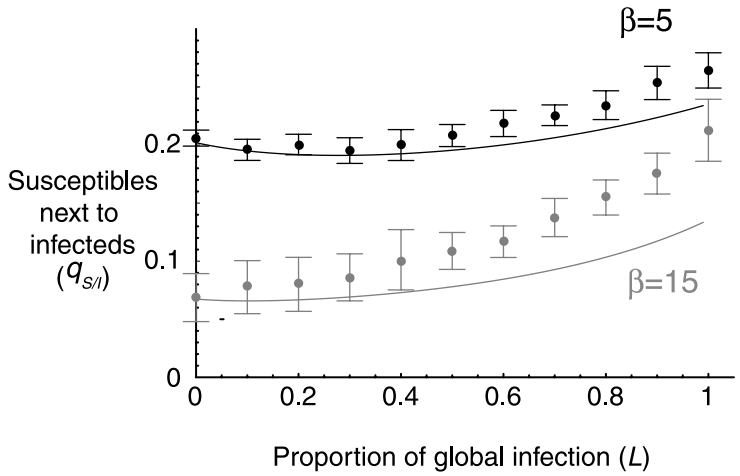

Fig. 3. The dependency of $q_{S/I}$ as a function of the proportion of global transmission when $\beta = 5$ (black) and $\beta = 15$ (grey) without any trade-offs. The lines indicate $q_{S/I}$ computed numerically using equations (A1), while the dots are the means of 20 Monte Carlo simulations (bars indicate standard deviations). Generally, because of self-shading, large L increases $q_{S/I}$. When $\beta = 5$ there is some evidence for the approximations of a minimum in $q_{S/I}$. With such small parameters, the global density of the susceptible individuals is larger than that of infected individuals and infected individuals are free from the self-shading. In any case, the effect is rather small in the simulations.

higher proportion of infecteds next to susceptibles ($q_{S/I}$) are at an advantage. In Fig. 3, we solve equations (A1) at steady state to show how $q_{S/I}$ changes with the proportion of global infection (L). There is generally an increase in $q_{S/I}$ as L increases, which suggests an evolutionary advantage in increasing the proportion of global infection. When transmission rates are low, there is some evidence that $q_{S/I}$ can be increased slightly at close to completely local transmission ($L \to 0$). This effect is less pronounced in simulations than in the approximations (Fig. 3), but may result from the fact that the global proportion of infecteds is lower than that of susceptibles and therefore little self-shading occurs. In general, however, there is a benefit to be gained in terms of increasing $q_{S/I}$ as long-distance infection rates are increased. This benefit is countered, however, by a cost to global infection due to the clustered nature of the host population. Figure 4A shows snapshots of the relatively sparse and filled landscapes that are produced by relatively low and high reproductive rates respectively. As the reproductive rate increases, space is filled up and, as shown in Fig. 4B, the ES proportion of global transmission also increases.

DISCUSSION

The evolution of optimal parasite dispersal

A combination of analytical approximation analysis and Monte Carlo simulation has shown that there is an evolutionarily stable proportion of global infection. Since we do not assume any direct costs of global transmission, one might think that the global infection would be always favoured by selection. It is well known that in homogeneous well-mixed populations, dispersal is always beneficial unless there is an explicit cost of dispersal, since it

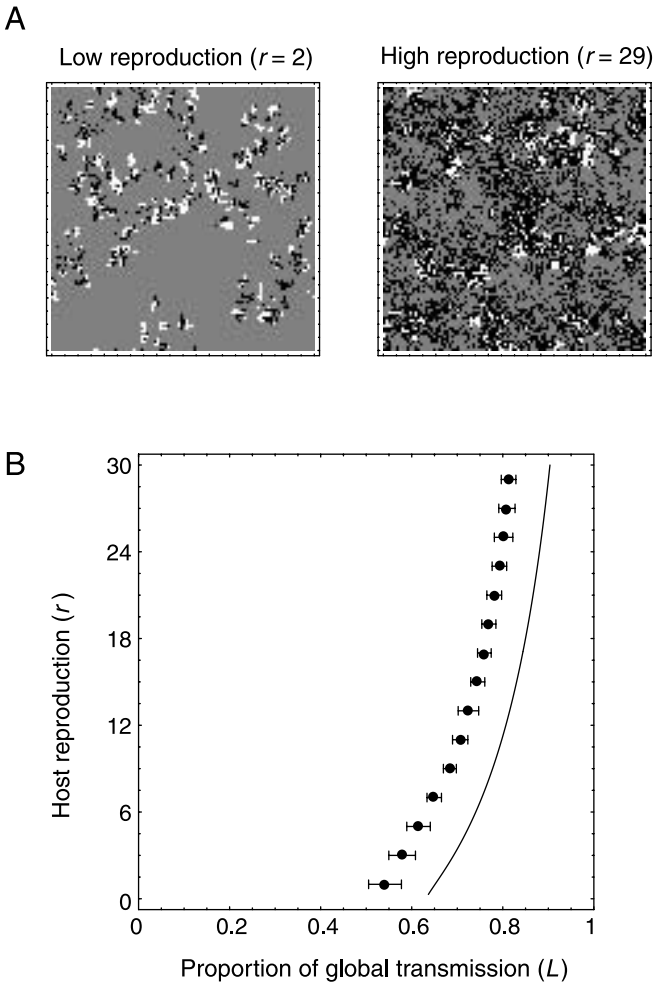

Fig. 4. (A) Snapshots of the lattice when $r = 2$ (left) and $r = 29$ (right). Black indicates infected individuals, white indicates susceptible individuals, and grey indicates empty sites. (B) The effect of reproduction rate on the ES proportion of global transmission. The vertical axis shows reproduction rate and the horizontal axis shows the proportion of global transmission. The line shows the ES proportion of global transmission. Dots show mean proportions of 20 Monte Carlo simulations (bars denote standard deviations). In the simulation, transmission rate is fixed at 10. When r is large, evolution leads to more global infection. Other parameters are as in Fig. 1.

reduces local competition (Hamilton and May, 1977; van Baalen and Rand, 1998; Harada, 1999; Rousset and Gandon, 2002). In the context of evolutionary epidemiology, this local competition occurs because local infection leads to 'self-shading' where locally there are high proportions of infected individuals. In our study, an optimal rather than maximal level of dispersal occurs because reproduction by susceptible individuals is always local and therefore a spatially heterogeneous resource (susceptibles) environment emerges for the parasite. This heterogeneity, which is only due to the assumption of local reproduction, leads to an emergent cost of dispersal. The effect is clearly demonstrated in Fig. 4, where the ES proportion of

global infection increases as the space fills up. Since most hosts will show such heterogeneity in nature, parasites will never be selected to disperse globally. Furthermore, we would predict that parasites will disperse further if their host population is spatially structured, but relatively homogeneous. Crop monocultures may be an extreme example of this type of host.

The optimal dispersal rate depends on the absolute transmission rate of the parasite. Higher transmission rates lead to more local transmission. This effect saturates so that increasing transmission to very high levels leads to approximately 50 : 50 global to local infection. In a spatial population, the key quantities that influence parasite fitness are the standard R_0 and the local density of susceptibles next to infecteds q_{SI}. Figure 3 shows how q_{SI} increases as the proportion of global infection increases. Note that this increase is more pronounced with higher absolute transmission rates. As a consequence of this effect, at higher absolute transmission rates there is more to be gained from dispersal. However, we have shown that increased transmission rates select for lower dispersal. This is because q_{SI} becomes less important once most of the infections are global. Also, high transmission rates lead to a higher degree of infection and therefore deaths due to infection. This in turn leads to a sparser population and therefore higher dispersal costs. A prediction of our model therefore is that parasites with high transmission rates may be selected to be more locally dispersing. This tends to make them more manageable.

Spatial structure and the evolution of parasite life histories

Our results provide further insights into the role of spatial structure in the evolution of parasite life histories. When the transmission rate and the proportion of global infection are allowed to evolve, maximum transmission is favoured if transmission rate and virulence are not linked. This maximization occurs at an intermediate proportion of global infection. The implication of this is that when parasites are able to evolve to alter their dispersal, they will maximize their transmission rate, even when their host population is clustered. Furthermore, after evolution to maximal transmission rate, about 50% of the infection events will still be local. Despite this, transmission is still maximized. These results suggest that local infection may well constrain the evolution of transmission rate (Rand *et al.*, 1995; Boots and Sasaki, 1999; Haraguchi and Sasaki, 2000), but not if the parasite is able to evolve its proportion of local/global transmission.

We also considered the concurrent evolution of dispersal and transmission when there is an accelerating cost to transmission through a trade-off with parasite virulence (Fig. 2B). This assumption lies at the heart of most of the evolution of virulence theory (Mackinnon and Read, 1999) and results in an ES finite transmission rate and virulence in completely mixed populations. Recent work (Kamo *et al.*, in press) has also shown that when the proportion of global transmission is fixed, highly local interactions lead to a lower ES transmission and virulence than in the mixed model. However, transmission and virulence increase at intermediate proportions of global infection, with their highest values again close to the ES proportion of global infection found in this paper. As such, parasites that are constrained by the standard transmission–virulence trade-off can also evolve their parasite dispersal rates and they will evolve to be more virulent than predicted in the mean-field. Our results, therefore, further emphasize the importance of considering spatial/population structure in evolutionary scenarios. More fundamentally, they emphasize that just comparing local and completely mixed models can be misleading. If the degree of local interaction is fixed,

completely spatial infection always leads to lower transmission and virulence (Rand *et al.*, 1995; Haraguchi and Sasaki, 2000; Boots and Sasaki, 1999; Kamo *et al.*, in press). This is true for all the trade-off shapes that we have considered here (Kamo *et al.*, in press). However, if the degree of local to global infection can evolve, unconstrained transmission is always maximized. When there is an ES transmission and virulence in the mean-field, evolution of the parasite dispersal rate leads to higher rather than lower transmission and virulence. These results only become apparent because we have considered models between the local and the global cases.

Pair approximations as a tool for understanding evolutionary dynamics

There has been considerable interest in the role of spatial structure in ecology and evolution (Dieckmann *et al.*, 2000). However, most evolutionary studies rely only on Monte Carlo simulations. By developing an approximate analytical technique in addition to the Monte Carlo simulation, we have been able to understand the evolutionary processes in our model in much more detail. The application of our approach may also allow a more complete understanding of the role of spatial structure in a wider range of evolutionary contexts. One limitation of our analysis, however, is that we largely rely on pair-approximation methods, and hence the analysis may not be accurate in all circumstances. However, approximations have been successfully used in a range of ecological and evolutionary scenarios (Harada and Iwasa, 1994, 1996; Harada *et al.*, 1995; Kubo *et al.*, 1996; Nakamaru *et al.*, 1997, 1998; Iwasa *et al.*, 1998; Harada, 1999; reviewed by Iwasa, 2000; Sato and Iwasa, 2000). For example, in a related study, Harada (1999) considered the evolution of ESS allocation rate between long- and short-range reproduction in plants. Her analysis used pair approximation and Monte Carlo simulations to draw PIPs and also found the evolution of a mixture of long- and short-range reproduction. When there is no cost for long-distance dispersal, Harada (1999) found that short-range reproduction does not evolve. In contrast, we do not assume any explicit cost for long-distance dispersal, but evolution still favours the evolution of a proportion of local and global transmission. Furthermore, Harada (1999) found that increased resources lead to more short-range dispersal. In contrast in our study, higher reproduction rates, which lead to more susceptible individuals and therefore resources for the pathogen, lead to more global transmission (Fig. 4). In both these studies, pair approximation works very well in terms of predicting the qualitative outcomes and, in particular, the existence of evolutionary attractors. Given the complexity of spatial models in general, theoretical progress is likely to be much more rapid with the adoption of these approximate analytical approaches.

All of the costs and benefits in our model emerge from the spatio-temporal ecology of the system. This emphasizes the importance of considering ecological dynamics in evolutionary models. The costs to local infection can be understood through general arguments associated with avoiding local competition, while the costs to global infection can in turn be understood by the more general phenomenon of heterogeneity in resources (Ferriere and Galliard, 2001). However, this heterogeneity is normally considered to be intrinsic to the environment, whereas here it emerges from the simple ecological interaction. In general, it is always important to consider evolutionary constraints such as these that arise from ecological characteristics of the systems themselves (Ferriere and Galliard, 2001).

When we consider the dispersal of parasites, it is clear that this will usually be one of the most dangerous parts of their life-cycle. Due to the difficulties of measuring dispersal, relatively little is known about the success rate of parasite dispersal stages. That said, when

they have been measured, dispersal costs have been shown to be substantial (Ward *et al.*, 1998). If there are indeed substantial survival costs associated with long-distance infection, selection is likely to lead to a greater proportion of local infection than we have shown in this paper. Since dispersal survival costs will tend to reduce the ES proportion of global transmission, they may also decrease ES transmission and virulence rates. Dispersal costs may therefore help to constrain parasite virulence. It also follows that the reduction of long-distance transmission events is likely to have evolutionary as well as epidemiological benefits in the management of disease.

ACKNOWLEDGEMENTS

We thank the Royal Society and JSPS for funding and Dylan Childs, Steve Webb, and Diana Bowler for comments on the manuscript.

REFERENCES

Bolker, B.M. 1999. Analytic models for the patchy spread of plant disease. *J. Math. Biol.*, **61**: 849–874.

Bolker, B.M. 2003. Combining endogenous and exogenous spatial variability in analytical population models. *Theor. Popul. Biol.*, **64**: 255–270.

Bolker, B. and Pacala, S.W. 1997. Using moment equations to understand stochastically driven spatial pattern formation in ecological systems. *Theor. Popul. Biol.*, **52**: 179–197.

Bolker, B.M. and Pacala, S.W. 1999. Spatial moment equations for plant competition: understanding spatial strategies and the advantages of short dispersal. *Am. Nat.*, **153**: 575–602.

Boots, M. and Sasaki, A. 1999. 'Small worlds' and the evolution of virulence: infection occurs locally and at a distance. *Proc. R. Soc. Lond. B*, **266**: 1933–1938.

Boots, M., Kamo, M. and Sasaki, A. 2006. Mathematical analysis by approximation: limits and directions. In *Disease Evolution: Models, Concepts, and Data Analyses* (Z. Feng, U. Dieckmann and S. Levin, eds.), pp. 3–21. Providence, RI: American Mathematical Society.

Bremermann, H.J. and Thieme, H.R. 1989. A competitive exclusion principle for pathogen virulence. *J. Math. Biol.*, **27**: 179–190.

Dieckmann, U., Law, R. and Metz, J.A.J., eds. 2000. *The Geometry of Ecological Interactions: Simplifying Spatial Complexity*. Cambridge: Cambridge University Press.

Ellner, S.P. 2001. Pair approximation for lattice models with multiple interaction scales. *J. Theor. Biol.*, **210**: 435–447.

Ewald, P.W. 1994. *Evolution of Infectious Disease*. Oxford: Oxford University Press.

Ferriere, R. and Galliard, J.F.L. 2001. Invasion fitness and adaptive dynamics in spatial population models. In *Dispersal* (J. Clobert, E. Danchin, A.A. Dhondt and J.D. Nichols, eds.), pp. 57–79. Oxford: Oxford University Press.

Ferriere, R. and Michod, R. 1995. Invading wave of cooperation in a spatial iterated prisoners dilemma. *Proc. R. Soc. Lond. B*, **259**: 77–83.

Ferriere, R. and Michod, R. 1996. The evolution of cooperation in spatially heterogeneous populations. *Am. Nat.*, **147**: 692–717.

Geritz, S., Metz, J.A.J., Kisdi, E. and Meszena, G. 1997. Dynamics of adaptation and evolutionary branching. *Phys. Rev. Lett.*, **78**: 2024–2027.

Geritz, S., Kisdi, E., Meszena, G. and Metz, J.A.J. 1998. Evolutionarily singular strategies and the adaptive growth and branching of the evolutionary tree. *Evol. Ecol.*, **12**: 35–57.

Hamilton, W.D. and May, R.M. 1977. Dispersal in stable habitats. *Nature*, **269**: 578–581.

Harada, Y. 1999. Short vs. long range disperser: the evolutionarily stable allocation in a lattice structured habitat. *J. Theor. Biol.*, **201**: 171–187.

Harada, Y. and Iwasa, Y. 1994. Lattice population dynamics for plants with dispersing seeds and vegetative propagation. *Res. Popul. Ecol.*, **36**: 237–249.

Harada, Y. and Iwasa, Y. 1996. Analyses of spatial patterns and population processes of clonal plants. *Res. Popul. Ecol.*, **38**: 153–164.

Harada, Y., Ezoe, H., Iwasa, Y., Matsuda, H. and Sato, K. 1995. Population persistence and spatially limited social interaction. *Theor. Popul. Biol.*, **48**: 65–91.

Haraguchi, Y. and Sasaki, A. 2000. The evolution of parasite virulence and transmission rate in a spatially structured population. *J. Theor. Biol.*, **203**: 85–96.

Iwasa, Y. 2000. Lattice models and pair approximation. In *The Geometry of Ecological Interactions: Simplifying Spatial Complexity* (U. Dieckmann, R. Law and J.A.J. Metz, eds.), pp. 227–251. Cambridge: Cambridge University Press.

Iwasa, Y., Nakamaru, M. and Levin, S.A. 1998. Allelopathy of bacteria in a lattice population: competition between colicin sensitive and colicin producing strains. *Evol. Ecol.*, **12**: 785–802.

Kamo, A., Sasaki, A. and Boots, M. 2006. The role of trade-off shapes in the evolution of parasites in spatial host populations: an approximate analytical approach. *J. Theor. Biol.* (DOI: 10.1016/j.jtbi.2006.08.013).

Kubo, T., Iwasa, Y. and Furumoto, N. 1996. Forest spatial dynamics with gap expansion: total gap area and gap size distribution. *J. Theor. Biol.*, **180**: 229–246.

Mackinnon, M. and Read, A.F. 1999. Selection for high and low virulence in the malaria parasite *Plasmodium chabaudi. Proc. R. Soc. Lond. B*, **266**: 741–748.

Matsuda, H., Ogita, N., Sasaki, A. and Sato, K. 1992. Statistical mechanics of population – the lattice Lotka-Volterra model. *Prog. Theor. Phys.*, **88**: 1035–1049.

May, R.M. and Anderson, R.M. 1983. Epidemiology and genetics in the coevolution of parasites and hosts. *Proc. R. Soc. Lond. B*, **219**: 281–313.

Murrell, D.J., Purves, D.W. and Law, R. 2001. Uniting pattern and process in plant ecology. *Trends Ecol. Evol.*, **16**: 529–530.

Murrell, D.J., Purves, D.W. and Law, R. 2002. The evolution of dispersal distance in spatially structured populations. *Oikos*, **97**: 229–236.

Murrell, D.J., Dieckmann, U. and Law, R. 2004. On moment closures for population dynamics in continuous space. *J. Thoer. Biol.*, **229**: 421–432.

Nakamaru, M., Matsuda, H. and Iwasa, Y. 1997. The evolution of cooperation in a lattice structured population. *J. Theor. Biol.*, **184**: 65–81.

Nakamaru, M., Nogami, H. and Iwasa, Y. 1998. Score dependent fertility model for the evolution of cooperation in a lattice. *J. Theor. Biol.*, **194**: 101–124.

Poulin, R. 1994. Metaanalysis of parasite induced behavioral changes. *Anim. Behav.*, **48**: 137–146.

Poulin, R. 1995. 'Adaptive' changes in the behaviour of parasitized animals: a critical review. *Int. J. Parasitol.*, **25**: 1371–1383.

Perez-Tris, J. and Bensch, S. 2005. Dispersal increases local transmission of avian malarial parasites. *Ecol. Lett.*, **8**: 838–845.

Rand, D., Keeling, M. and Wilson, H.B. 1995. Invasion, stability and evolution to criticality in spatially extended, artificial host pathogen ecologies. *Proc. R. Soc. Lond. B*, **259**: 55–63.

Rhodes, C.J. and Anderson, R.M. 1996. Dynamics in a lattice epidemic model. *Phys. Lett. A*, **210**: 183–188.

Rousset, F. and Gandon, S. 2002. Evolution of the distribution of dispersal distance under distance dependent cost of dispersal. *J. Thoer. Biol.*, **15**: 515–523.

Sato, K. and Iwasa, Y. 2000. Pair approximations for lattice-based ecological models. In *The Geometry of Ecological Interactions: Simplifying Spatial Complexity* (U. Dieckmann, R. Law and J.A.J. Metz, eds.), pp. 341–358. Cambridge: Cambridge University Press.

Sato, K., Matsuda, H. and Sasaki, A. 1994. Pathogen invasion and host extinction in lattice structured populations. *J. Math. Biol.*, **32**: 251–268.

van Baalen, M. and Rand, D.A. 1998. The unit of selection in viscous populations and the evolution of altruism. *J. Theor. Biol.*, **193**: 631–648.

Ward, S.A., Leather, S.R., Pickup, J. and Harrington, R. 1998. Mortality during dispersal and the cost of host-specificity in parasites: how many aphids find hosts. *J. Anim. Ecol.*, **67**: 763–773.

APPENDIX 1: RESIDENT DYNAMICS

Here, we show the dynamics of hosts on the lattice. The definition of variables and transition rule are in the main text. The pair densities approximately change in time as

$$\begin{aligned}
\dot{P}_{OO} &= 2[dP_{SO} + (d+\alpha_I)P_{IO} - r(1-\theta)q_{S|OO}P_{OO}] \\
\dot{P}_{SO} &= dP_{SS} + (d+\alpha_I)P_{IS} - dP_{SO} + r(1-\theta)q_{S|OO}P_{OO} \\
&\quad - [r\{\theta + (1-\theta)q_{S|OS}\} + \beta_I\{L_I\rho_I + (1-L_I)(1-\theta)q_{I|SO}\}]P_{SO} \\
\dot{P}_{SS} &= -2[dP_{SS} + \beta_I\{L_I\rho_I + (1-L_I)(1-\theta)q_{I|SS}\}P_{SS}] + 2r\{\theta + (1-\theta)q_{S|OS}\}P_{SO} \\
\dot{P}_{IO} &= dP_{IS} + (d+\alpha_I)P_{II} - \{(d+\alpha_I) + r(1-\theta)q_{S|OI}\}P_{IO} \\
&\quad + \beta_I\{L_I\rho_I + (1-L_I)(1-\theta)q_{I|SO})\}P_{SO} \\
\dot{P}_{IS} &= -\{d + (d+\alpha_I)\}P_{IS} - \beta_I[L_I\rho_I + (1-L_I)\{\theta + (1-\theta)q_{I|SI}\}]P_{IS} \\
&\quad + r(1-\theta)q_{S|OI}P_{IO} + \beta_I\{L_I\rho_I + (1-L_I)(1-\theta)q_{I|SS}\}P_{SS} \\
\dot{P}_{II} &= -2(d+\alpha_I)P_{II} + 2\beta_I[L_I\rho_I + (1-L_I)\{\theta + (1-\theta)q_{I|SI}\}]P_{IS}
\end{aligned} \tag{A1}$$

where $\dot{x}$ is the time derivative of x. All parameters related to the pathogen's life-history traits have a subscript I. L_I is the proportion of global infection. β_I, α_I, d, and r are the transmission rate, virulence, natural death rate, and growth rate respectively. $\theta = 1/z$ where z is the number of neighbouring sites, which is 4 in our study.

APPENDIX 2: MUTANT DYNAMICS

Here, we show the mutant dynamics to obtain the quasi-equilibrium values. An example of the derivation of the mutant dynamics is shown in the main text. We use the identity relationships in equation (1) and the standard linearization technique to derive these equations.

$$\begin{aligned}
\dot{q}_{O|J} &= dq_{S|J} + (d+\alpha_I)q_{I|J} + (d+\alpha_J)q_{J|J} - r(1-\theta)q_{S|O}q_{O|J} \\
&\quad + \beta_J[L_J\rho_S + (1-L_J)(1-\theta)q_{S|J}]q_{O|S} - \beta_J[L_J\rho_S + (1-L_J)q_{S|J}]q_{O|J} \\
\dot{q}_{S|J} &= -dq_{S|J} + r(1-\theta)q_{S|O}q_{O|J} - \beta_I[L_I\rho_I + (1-L_I)(1-\theta)q_{I|S}]q_{S|J} \\
&\quad + \beta_J[L_J\rho_S + (1-L_J)(1-\theta)q_{S|J}]q_{S|S} - \beta_J\theta(1-L_J)q_{S|J} \\
&\quad - \beta_J[L_J\rho_S + (1-L_J)q_{S|J}]q_{S|J}, \\
\dot{q}_{I|J} &= -(d+\alpha_I)q_{I|J} + \beta_I[L_I\rho_I + (1-L_I)(1-\theta)q_{I|S}]q_{S|J}
\end{aligned}$$

$$+\beta_J[L_J\rho_S+(1-L_J)(1-\theta)q_{SIJ}]q_{IIS}-\beta_J[L_J\rho_S+(1-L_J)q_{SIJ}]q_{IIJ}$$

$$\dot{q}_{JIJ}=-(d+\alpha_J)q_{JIJ}+2\beta_J\theta(1-L_J)q_{SIJ}-\beta_J[L_J\rho_S+(1-L_J)q_{SIJ}]q_{JIJ} \quad \text{(A2)}$$

Note that all the conditional probabilities without J (e.g. q_{IIS}) are equilibrium values computed from equations (A1) and are therefore constants. We can solve these equations numerically and the quasi-equilibrium value, $\hat{q}^0_{SIJ}$, is obtained. Using the value we can determine the invadability of the mutant from equation (4).